MLM-2627(OP)
CONF-790907--6

SURFACE STUDIES OF AN ALUMINUM/CUPROUS OXIDE THERMITE MIXTURE BY X-RAY PHOTOELECTRON AND AUGER SPECTROSCOPIES

I. Studies of Aluminum

W. E. Moddeman and A. Rengan
University of Dayton Research Institute
and
Materials Engineering Graduate Program,
School of Engineering
University of Dayton
Dayton, Ohio 45342

and

P. S. Wang and L. D. Haws
Monsanto Research Corporation
Mound Facility
Miamisburg, Ohio 45342

ABSTRACT

Thermite is a name given to a mixture of powdered metal and a metallic oxide. The thermite under examination was a powdered mixture of aluminum metal and cuprous oxide in a mole ratio of 2:3. The surface chemistries of the powdered aluminum and the thermite mixture were examined by the surface analysis techniques of X-ray photoelectron spectroscopy (XPS) and high resolution Auger electron spectroscopy (AES). Surface characterization with XPS and AES found the presence of carbon and aluminum oxide on the aluminum reactant and mixtures. A surface oxide thickness of 9.8 Å was measured for room temperature stored powdered aluminum metal. The aluminum oxide thickness on the aluminum powder was noted to be larger for room temperature aged thermite powder (10.5 Å) and a thermite pressed pellet (22 Å). All oxide thicknesses were found to be larger when aged in dry air or argon at an elevated temperature of 180°C. The largest oxide thickness measured was 26 Å. Carbon contaminant levels were measured and were found to decrease from 64 Å for room temperature stored metal to 34 Å for metal stored at 180°C.

---

1. INTRODUCTION

When a thermite mixture is ignited the chemical reaction proceeds rapidly with a great evolution of heat.[1] The thermite process is based on the fact that a metal with a large oxidation potential, such as aluminum, has a great affinity for oxygen of a metal oxide, such as cuprous or iron oxides.

The thermite mixture being studied consists of a Reynolds XD28 flake aluminum and a Cerac "Pure" cuprous oxide powder. They are mixed in a metal to oxide weight ratio of 1:8 formulation. The mixture is not explosive, and can only be ignited after a temperature of ∿1540°C is reached. Once ignited, temperatures in excess of 2400°C are achievable. The reaction is $2Al + 3Cu_2O \rightarrow 6Cu + Al_2O_3$ with a large negative change in the enthalpy of 218 kcal/mole. There has recently been considerable interest in the compatibility of reactants in thermite materials and a study of the surface chemistry of the aluminum is reported in this paper.

2. EXPERIMENTAL PROCEDURE AND TECHNIQUES

High purity, powdered aluminum metal and cuprous oxide were stored in evacuated, heat treated, and flushed Pyrex test tubes. Two storage atmospheres were used, dry air and argon. Cuprous oxide was initially sieved through a 400-mesh screen to remove large particles.* Aluminum powders were used as received. The thermite was made stoichiometrically and dry mixed for one hour in a V-blender to provide adequate homogeneity of the composite thermite powder.

The pellets were obtained by a consolidation procedure of pressing the thermite powdered mixture in preheated, highly

---

*Data on the copper chemistry will not be presented in these proceedings, but will be presented elsewhere.

polished, graphite dies which were contained under an atmosphere of dry nitrogen.[1] This pressing process produced cylindrical pellets of ∿6 mm in diameter and ∿2 mm in height. A Teflon coated razor blade was used for generating a fractured surface of a pellet.

The XPS spectrometer is a modified AEI ES-100 instrument. This spectrometer with the accompanying argon ion sputtering capability has been discussed in more detail elsewhere.[2] The system is pumped by two 250ℓ/sec diffusion pumps and a 260ℓ/sec turbomolecular pump. Vacuum achievable in the sample chamber is 10^{-8} Torr. The chamber is bakable to >150°C. Reactive vapors can be minimized in the system by baking, by using a Ti sublimation pump, and by two liquid N_2 cryostations. The anode used for all the XPS measurements was silicon.

3. RESULTS AND DISCUSSION

3.1. General Equations for Carbon and Oxide Thickness Measurements

X-ray photoelectron spectroscopy is a surface sensitive technique that can be used to obtain thickness values of thin films on the very sensitive monolayer level of coverage. The maximum depth of analysis with XPS is dependent on the mean free path of inelastically scattered photoelectrons through the solid. In the following discussion, the general equations that are used to obtain thickness information in XPS or AES are given. These equations will be used in the following sections to calculate the carbon and/or oxide film thicknesses on the thermite reactants Al and Cu_2O.

The mean free path of an electron in a solid increases with kinetic energy (above ∿50 eV).[3] In XPS the analyzed depth is dependent on the energy of the incident radiation. SiK_α X-rays have been used in this Al/Cu_2O thermite study to be able to excite Al 1s photo- and Al KLL Auger electrons. The XPS and the Auger processes are discussed elsewhere.[4-7]

The nearly free electron nature of aluminum metal shows a high affinity for atmospheric oxygen with the subsequent formation of an aluminum oxide layer. Surface exminations of the ambient oxide layer formed on aluminum metal have been measured and have been shown to vary from a few angstrom to ∿25 Å thick.[8] It is evident from this present study that a surface sensitive technique like XPS and AES can provide valuable information on film thicknesses in thermite materials.

The intensity, I, of electrons of a given energy in a homogeneous material can be expressed by the following relationship:[9]

$$dI = F\alpha A\kappa n \exp(-x/\lambda)dx$$

where F is the photon flux; α is the cross section for photoionization; A is the sample area from which the photoelectrons are detected; κ is the spectrometer transmission factor; n is the number of atoms of the element per cm^3, λ is the mean free path of the photoelectron, and x is the distance through the material that the inelastically scattered photoelectron must travel. The mean free path is dependent on (a) the kinetic energy of the photoelectron and (b) the nature of the sample medium through which it passes.

For a layer of "infinite" thickness, the total intensity is obtained by integrating from $o< x <\infty$:

$$\int_o^\infty dI = \int_o^\infty F\alpha A\kappa n \exp(-x/\lambda)dx \qquad (1)$$

or

$$I^* = F\alpha A\kappa n\lambda$$

for an ideal homogeneous medium.

In this study, the interested layer (or layers) was of finite thickness. The aluminum was found to be contaminated with an oxide film and a carbonaceous film. Figure 1 represents a layered system of metal/metal oxide/carbon. The thickness of the carbon

layer is d_C. Consider a carbon photoelectron, e_C, from a depth x where $0 < x < d_C$. The total carbon intensity from this finite layer is:

$$I_C = \int_0^{d_C} F\alpha A\kappa n_C \exp(-x/\lambda_C)\,dx \qquad \text{or}$$

$$I_C = F\alpha A\kappa n_C \lambda_C \,[1-\exp(-d_C/\lambda_C)].$$

and, combining with Equation (1) gives:

$$I_C = I_C^* \,[1-\exp(-d_C/\lambda_C)] \qquad (2)$$

Similar equations can be written for the oxide layer and the metal substrate. These are given below:

$$I_O = I_O^* \,[\exp -d_C/(\lambda_O)_C]\,[1-\exp -d_O/\lambda_O] \qquad (3)$$

and

$$I_M = I_M^* \,[\exp -d_O/(\lambda_M)_O]\,[\exp -d_C/(\lambda_M)_C] \qquad (4)$$

The intensities of Auger lines and of photopeaks were measured from clean homogeneous substrates of the three materials, carbon, aluminum oxide, and aluminum metal. In these studies it was essential to minimize the number of variables associated with Equation (1). F was kept constant by means of a highly stabilized supply; A was kept at 5x5 mm^2, except when noted; α and λ are constants for a particular energy level and element; and κ remained constant during the entire study. Thus, $I^* \propto n$, the number of atoms of an element per cm^3.

Table I lists the λ values and I^* intensities for the various materials.

3.2. Thickness Measurements

Figures 1a and 1b illustrate the overall spectra excited by SiK_α radiation, 180°C aged for the flaked aluminum aged at 180°C, and for the thermite powder aged at 180°C. The main photopeaks are

TABLE I

MEAN FREE PATH VALUES IN ANGSTROMS AND MAXIMUM INTENSITY (I*) FOR THE ALUMINUM K-$L_{2,3}L_{2,3}$ AUGER, AND FOR THE ALUMINUM 2s AND CARBON 1s PHOTOELECTRONS

	Al K-LL		Al 2s		C 1s
	for oxide of 1385 eV	for metal of 1393 eV	for oxide of 1615 eV	for metal of 1618 eV	of 1454 eV
λ_C					94.9
$(\lambda_O)_C$	91.8		102.0		
$(\lambda_M)_C$		92.2		102.2	
λ_O	16.6		18.1		
$(\lambda_M)_O$		16.6		18.1	
I_C^*					890.0
I_O^*	5722.0		576.0		
I_M^*		4300.0		501.0	

λ_C is the mean free path of a carbon 1s photoelectron through a homogeneous carbon substance.

$(\lambda_O)_C$ is the mean free path of a photo- or Auger electron from aluminum of aluminum oxide through a homogeneous carbon film.

$(\lambda_M)_C$ is the mean free path of an aluminum metal photo- or Auger electron through a homogeneous carbon film.

λ_O is the mean free path of an aluminum oxide photo- or Auger electron through the oxide material itself.

$(\lambda_M)_O$ is the mean free path of an aluminum metal photo- or Auger electron through a homogeneous oxide layer.

I^* are given in counts-eV/sec. This unit is a triangular approximation to the area under a photoelectron or Auger peak. The photo or Auger peak height is measured in centimeters, converted to counts per second, and then multiplied by the full-width at half maximum in electron volts.

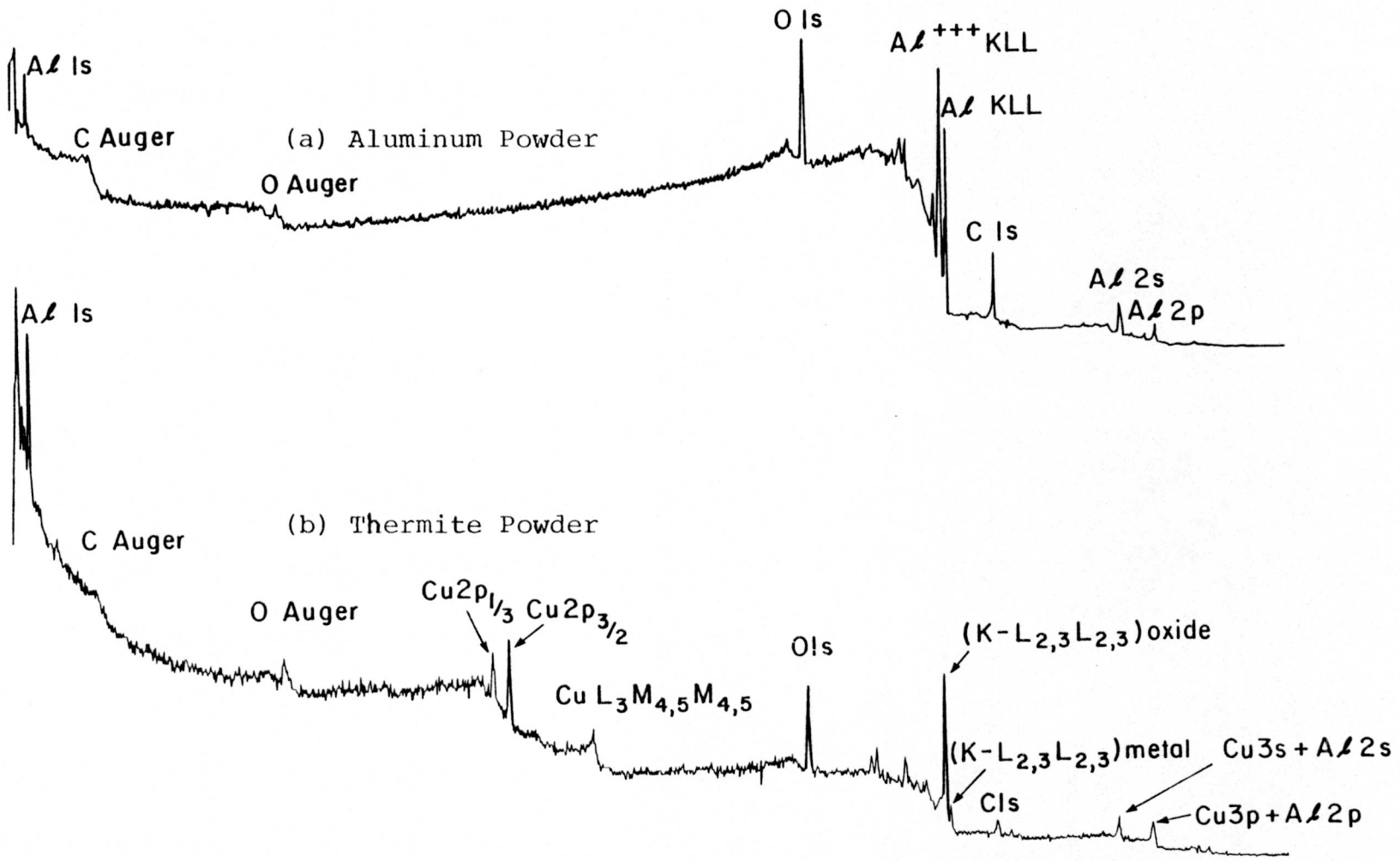

Figure 1. Overall XPS Spectra of (a) 180°C Aged Flaked Aluminum and (b) 180°C Aged Thermite Powdered Specimens. Both Spectra were Excited by SiK_{α} Radiation.

labeled in each spectrum. Photo- and Auger lines from copper, aluminum, and oxygen are observable as well as from carbon. Figure 2 illustrates the K-$L_{2,3}L_{2,3}$ scans for (a) aluminum oxide and (b) aluminum metal. Both the aluminum K-LL from the oxide and from the metal peaks have two normal Auger lines which are separated by 6 eV. These lines are due to different $2p^4$ final states.[6,10] In addition, the aluminum metal has a surface or bulk plasmon structure in the spectra. This plasmon structure is not found in photo-electron or Auger transitions in the oxide. Bulk plasmon losses occur as a result of a collective excitation of valence electrons occurring during photoionization of core levels or in the de-excitation of high energy states with core hole vacancies. These are observable at ∿15 eV from the main photo-

Figure 3 illustrates representative scans of the carbon 1s and aluminum K-LL Auger transition for air-aged aluminum powders. Figures 4 and 5 illustrate similar data for the thermite powder and pellet, respectively. By means of the data extracted from these Figures, the constants in Table I, and Equations (2), (3), and (4), carbon and oxide thicknesses can be calculated. The result of these calculations are summarized in Table II.

By comparing the oxide data, it can be concluded that the aluminum oxide thickness increases as a result of simply mixing the reactants to form the stoichiometric thermite powder. (Compare 9.8 to 10.5 Å increase noted for the room temperature air-aged aluminum powder and thermite powder.) This is better shown by comparing the results illustrated in Figure 6. In all cases, the oxide further thickens upon aging at 180°C in dry air. Also a larger increase in oxide thicknesses on aluminum can be noted in the aged thermite powder mixtures compared to aged aluminum powder material. Thus, it can be concluded that the increased oxide growth rate on aluminum in thermite powders is in great part due to oxygen transfer from the cuprous oxide to the aluminum metal.

From the data on the oxide thickness recorded on the pellets, one will conclude that the oxide thickness is substantially larger following the consolidation procedure on the thermite powder.

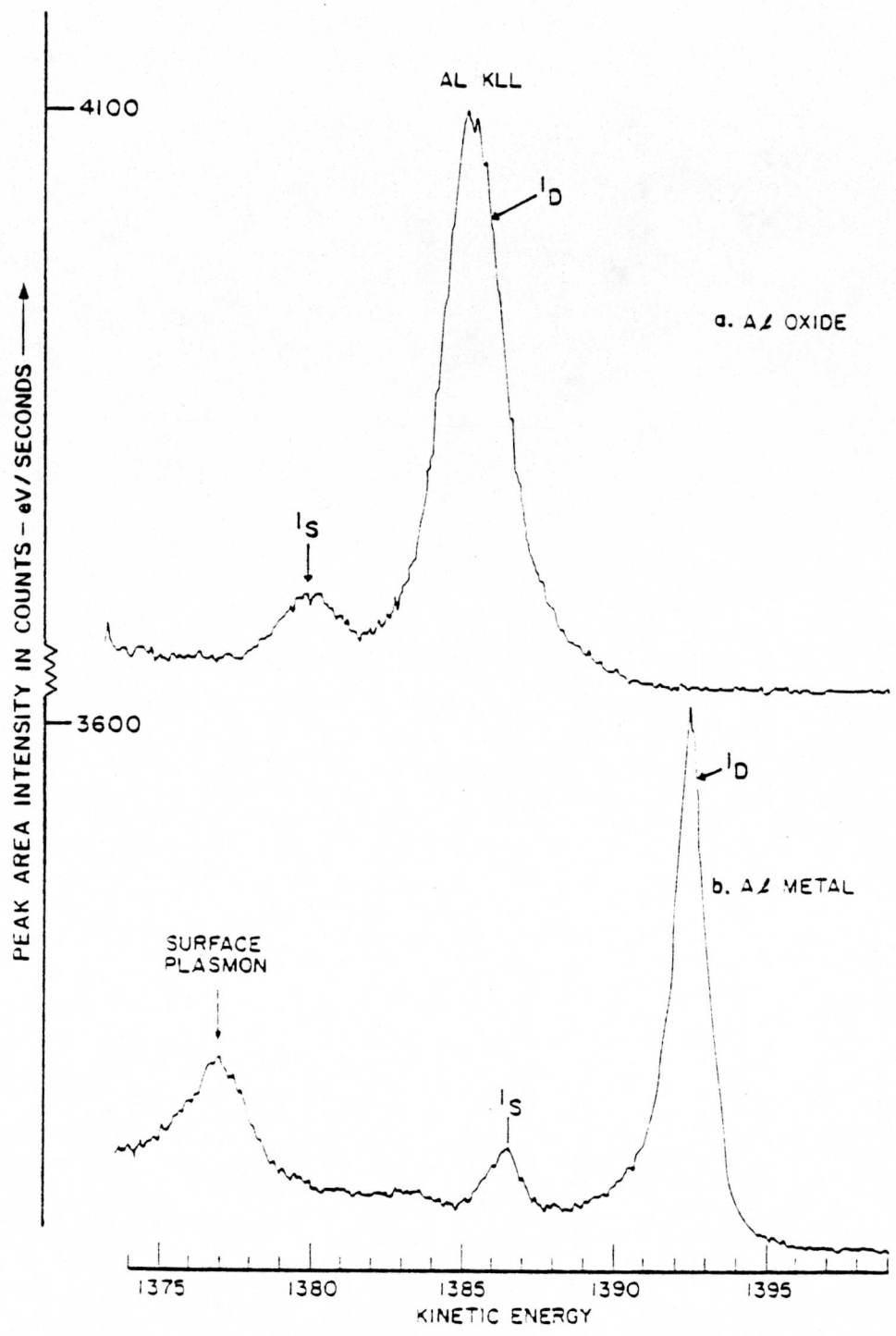

Figure 2. Aluminum K-$L_{2,3}L_{2,3}$ High Resolution Scans for: (a) Aluminum Oxide and (b) Aluminum Metal. The Strongest Auger Lines, at 1392 eV for Metal and 1385.5 eV for the Oxide, are due to a $1s^1 2s^2 2p^6 (^2S) \rightarrow 1s^2 2s^2 2p^4 (^1D)$ Transition. The Lines at 1386.5 eV for the Metal and 1380 eV for the Oxide are due to a $1s^1 2s^2 2p^6 (^2S) \rightarrow 1s^2 2s^2 2p^4 (^1S)$ Transition.

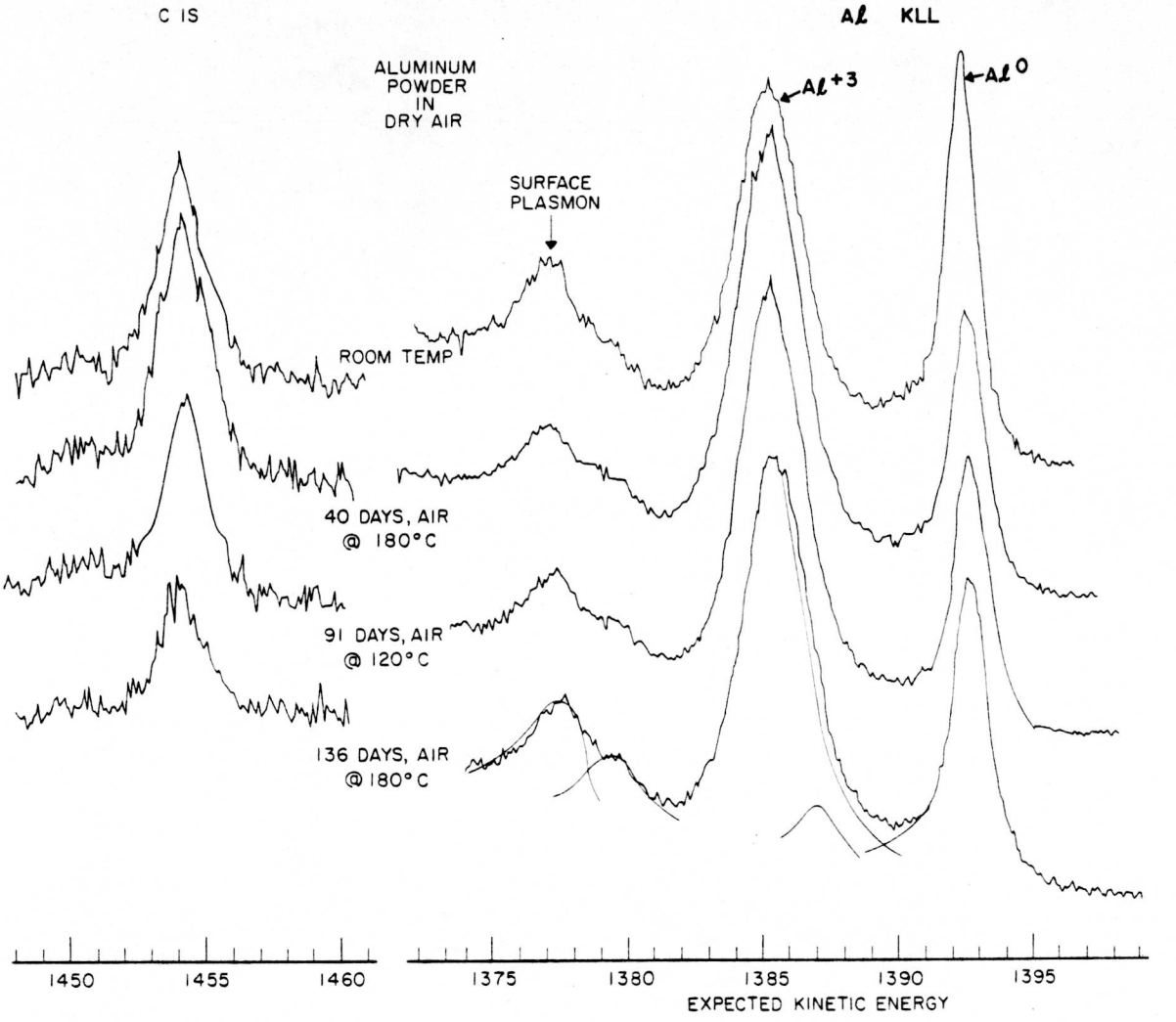

Figure 3. Representative Scans of Carbon 1s and Aluminum K-$L_{2,3}L_{2,3}$ Auger Transition for Aged Aluminum Powders in Dry Air at Different Temperatures. Auger and Photoelectron Lines Excited by SiK_{α} Radiation.

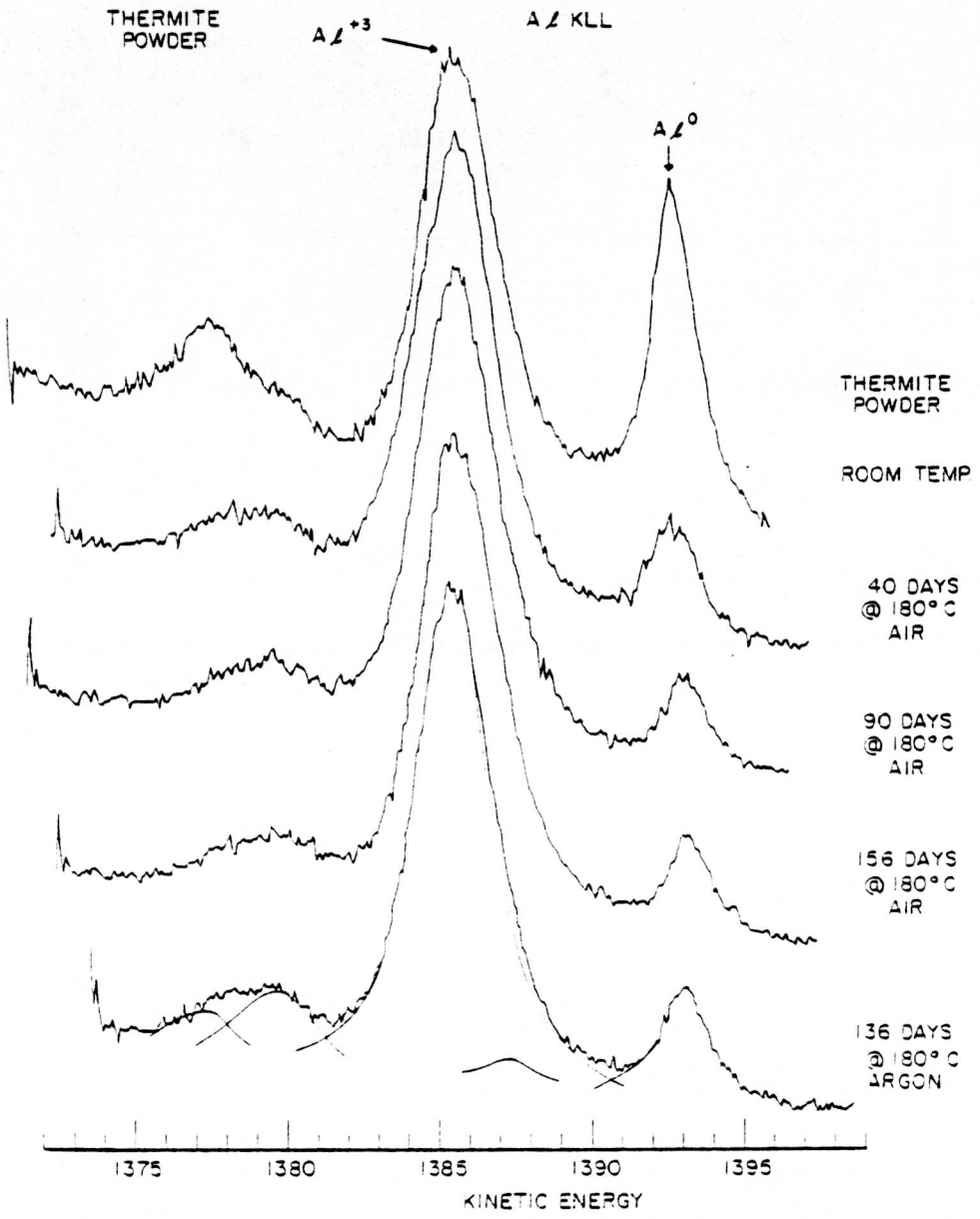

Figure 4. Representative Scans of Aluminum K-$L_{2,3}L_{2,3}$ Auger Peaks for Aged Thermite Powders.

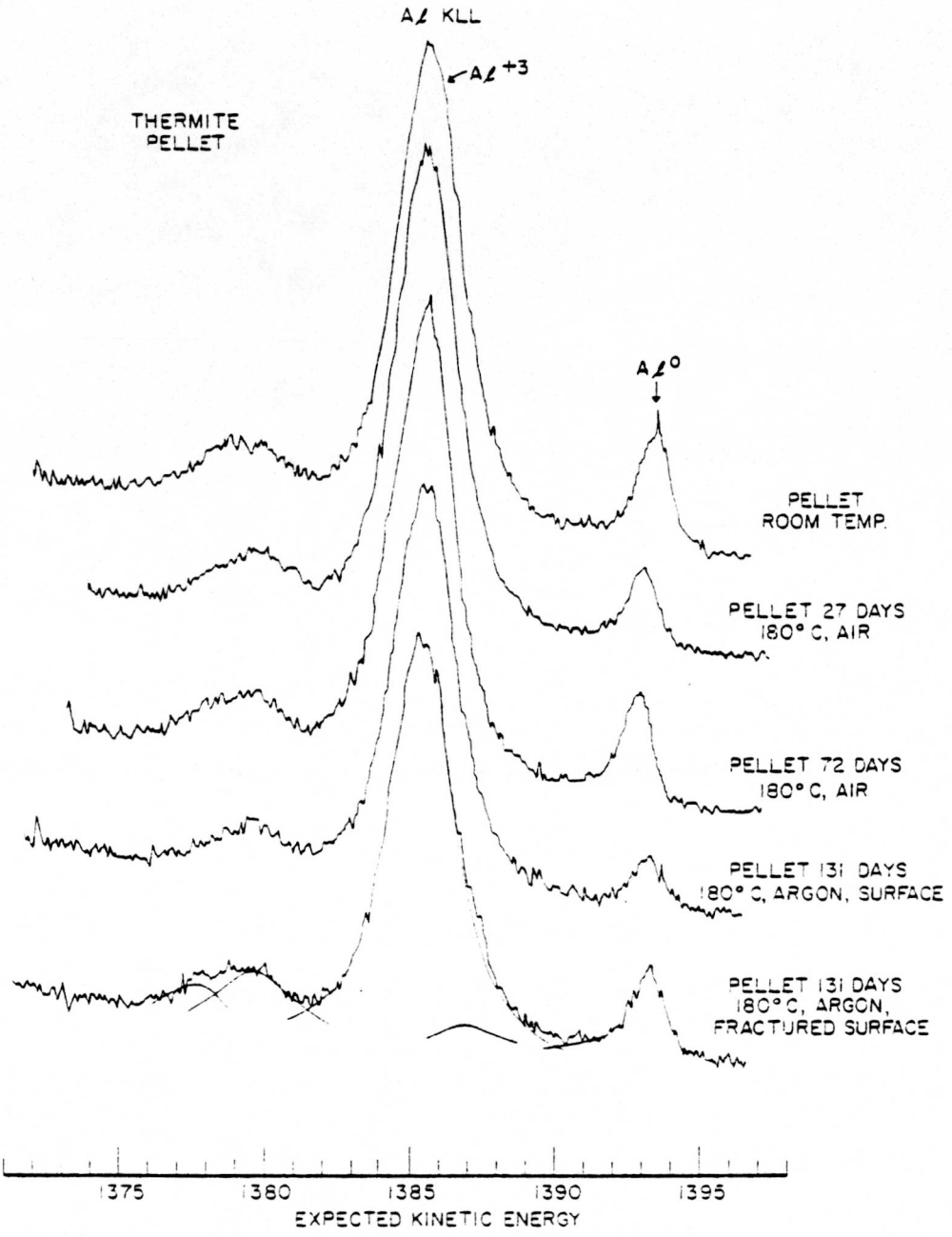

Figure 5. Representative Scans of Aluminum K-$L_{2,3}L_{2,3}$ Auger Transition Peaks for Aged Thermite Pellets.

TABLE II

SUMMARY OF CARBON AND OXIDE THICKNESSES IN ANGSTROMS MEASURED ON AIR-AGED AND ON ARGON-AGED ALUMINUM, THERMITE, AND PELLETS*

Sample	Condition	d_C	d_O
Aluminum Powder	Room Temp., Air-Aged	63	9.8
Aluminum Powder	40 days, 180°C., Air-Aged	47	13.2
Aluminum Powder	40 days, 180°C., Argon-Aged	20	12.2
Aluminum Powder	91 days, 180°C., Air-Aged	57	13.4
Aluminum Powder	91 days, 180°C., Argon-Aged	22	12.2
Aluminum Powder	136 days, 180°C., Air-Aged	34	13.2
Aluminum Powder	136 days, 180°C., Argon-Aged	23	12.8
Thermite Powder	Room Temp., Air-Aged		10.5
Thermite Powder	40 days, 180°C., Air-Aged		21.4
Thermite Powder	91 days, 180°C., Air-Aged		24.9
Thermite Powder	136 days, 180°C., Air-Aged		23.8
Thermite Powder	136 days, 180°C., Argon-Aged		22.4
Thermite Pellets	Room Temp., Air-Aged	11	22.4
Thermite Pellets	27 days, 60°C., Air-Aged	18	25.5
Thermite Pellets	27 days, 180°C., Air-Aged	15	26.1
Thermite Pellets	72 days, 180°C., Air-Aged	20	25.0
Thermite Pellets	Fractured Surface 27 days, 60°C., Air-Aged	12	23.7
Thermite Pellets	Fractured Surface 131 days, 180°C., Air-Aged	17	23.4

*Standard deviation measured for data given in the Table is ≤ 1 Å.

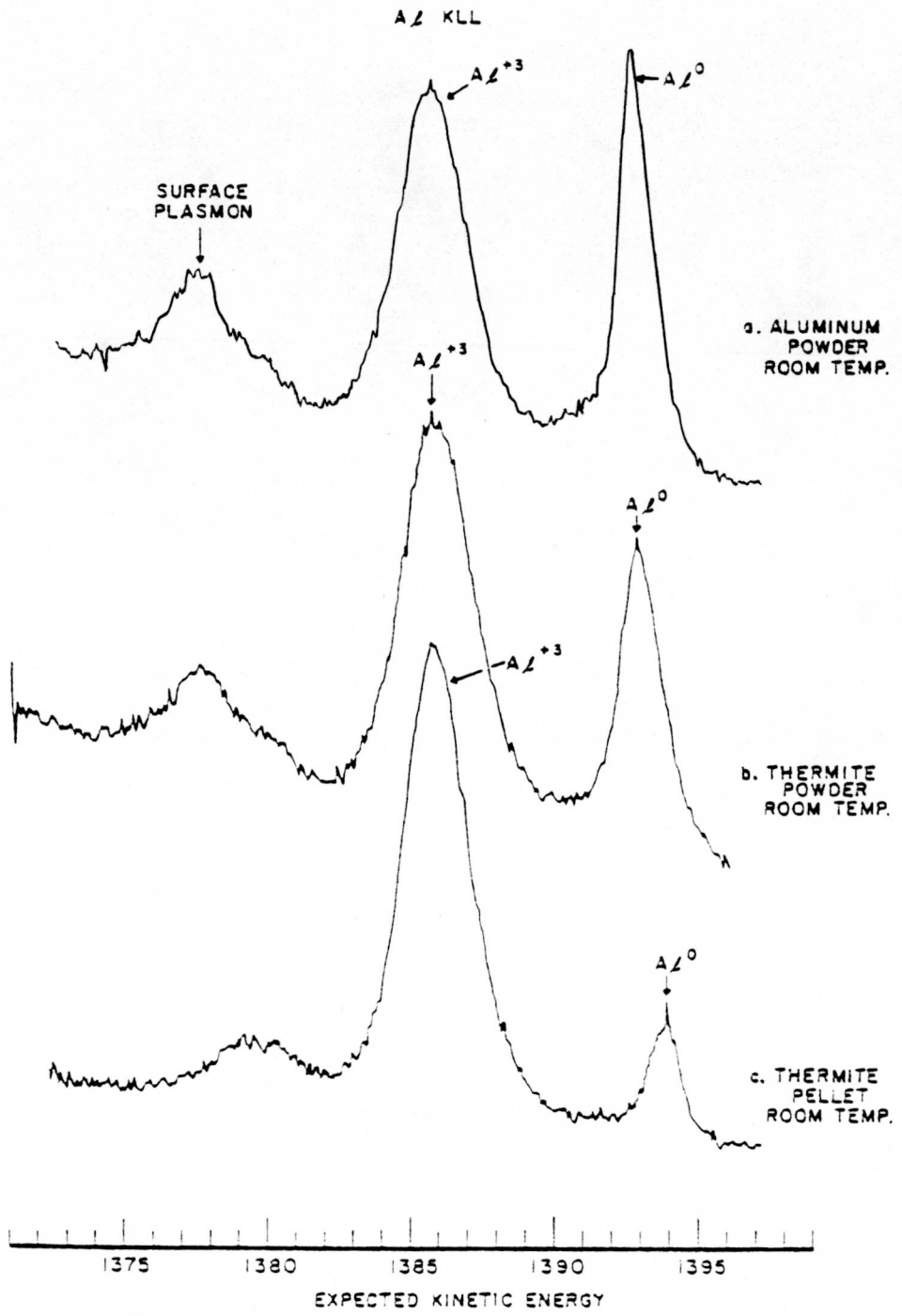

Figure 6. Comparison of the Aluminum K-$L_{2,3}L_{2,3}$ Auger Peaks for Room Temperature Aged: (a) Aluminum Powder, (b) Thermite Powdered Mixture, and (c) Thermite Pressed Pellet.

In Figure 7, the total intensity K-$L_{2,3}L_{2,3}$ aluminum intensity has been ratioed to the copper $2p_{3/2}$ photoelectron intensity and plotted against the time in days of aging in order to determine the possibility of surface diffusion in the pellet. As can be determined from the plot, there is an enrichment of aluminum on the pellet surface during the aging process.

3.3. Discussion of Error

The major sources of error in determining oxide and carbon thicknesses are inherent in the variables of Equation (1). These variables will be examined briefly. The photon flux was kept constant by a highly stabilized X-ray supply. The X-ray filament current was held at 5 mA and the anode potential at 10 kV. The rated stability of the supply is 0.2 percent. Although the variation in photon flux is directly proportional to variations in X-ray power, oftimes tungsten plating from the filament on the anode and/or X-ray window causes severe degradation in the characteristic photon flux reaching the sample. In this study the counting rate on Au $4f_{7/2}$ of an Ar ion cleaned gold specimen was measured prior to, during, and following the thermite study. Counting rates on Au varied <5 percent during the entire duration of the study. The net counting rate on the Au $4f_{7/2}$ was 760 ± 15 counts/sec above background. The full width at half maximum for this line was measured to be 1.2 eV. Also, to assure that the flux remained constant during the study, the condition of the anode and window were checked immediately following the thermite analysis. No tungsten discoloration could be noted on either the anode or window.

Other variables in Equation (1) are the spectrometer transmission function and the cross-section for photoionization. The spectrometer was set in a fixed analyzer transmission mode of operation. In this mode, the analyzer is fixed for detecting 65 eV electrons and the lens is varied in potential. All spectra were recorded in this mode of operation. For a particular level, the cross-section is constant and dependent only on the subshell excited and the photon source.

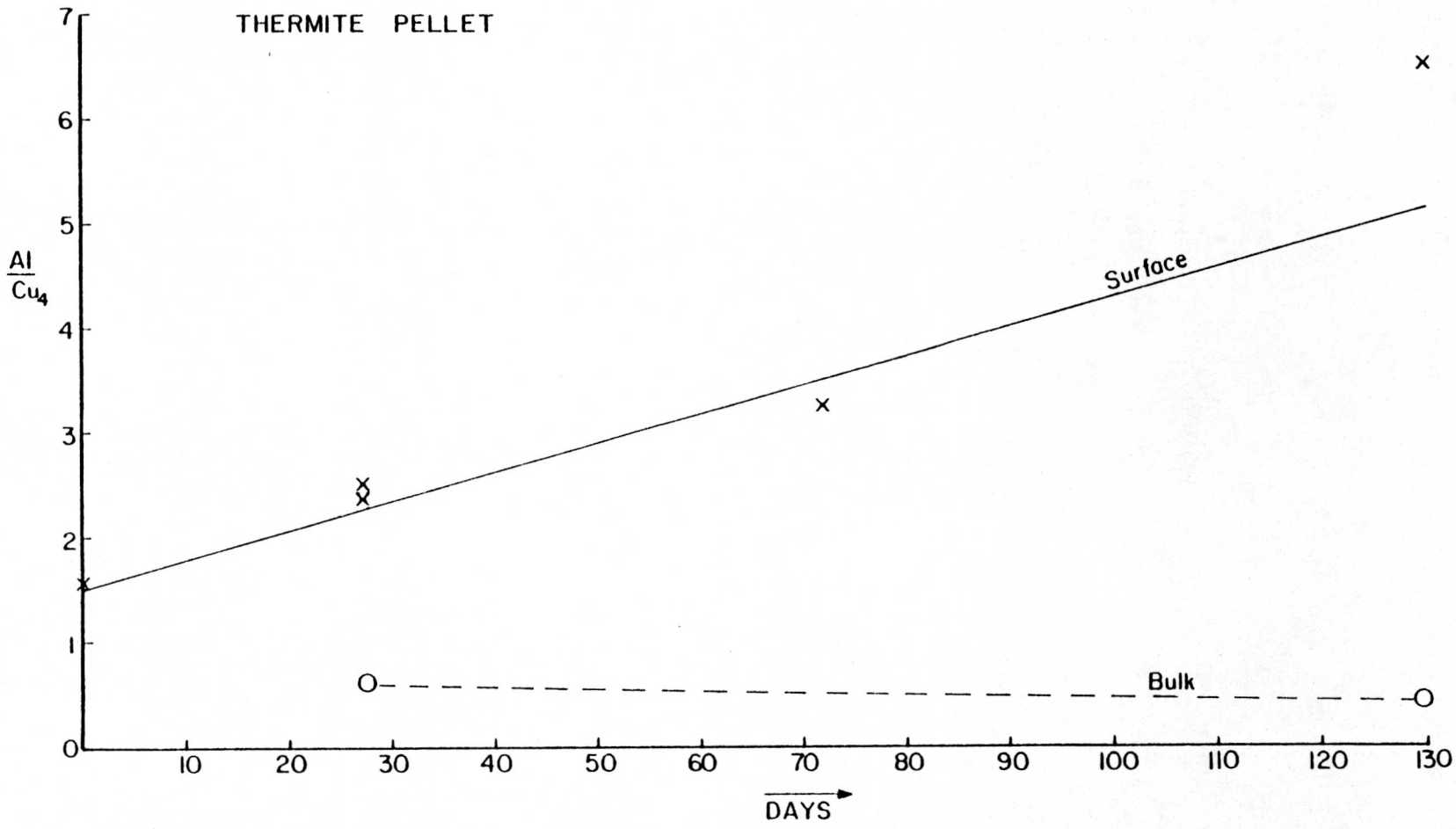

Figure 7. Ratio of the Aluminum K-$L_{2,3}L_{2,3}$ Auger Intensity to the Cu $2p_{3/2}$ Photoelectron Intensity for the Aged Thermite Pellets. Aging Temperature of 180°C.

The remaining variables of Equation (1) are the mean free path and sample area being analyzed. The use of the correct mean free path values can be the largest source of error in accurately determining oxide thickness. Mean free path values, λ, can be determined, however, only with great difficulty. In this study literature values of λ were used. These varied in quoted confidence. At 95 percent confidence the quoted λ values deviated by as much as 20 percent.

I_O values were measured for 5 x 5 mm^2 and 5 x 6 mm^2 fully oxidized specimens. For the limited amount of available data, a 25 percent increase in sample area corresponds to $\sim$30 percent increase in intensity in I_O. Perhaps more interesting are the I_O^* values and their standard deviations which reflects the reproducibility of the maximum intensities observable from aluminum of aluminum oxide. For five independent measurements, I_O^* was found to be 5722 $\pm$ 514 for the Al K-LL Auger peak, a standard deviation of 8.9 percent.

Other variables to be considered are errors in estimating background, changes in angular detection, interface structure and surface roughness. Each of these possible causes are addressed below.

The background observed with the standard materials, metal aluminum foil and the oxide grown on the foil, had a gradual sloping background, whereas, the background observed with the powdered specimens showed a significant increase in signal strength as the kinetic energy decreased. The increased sloping background with the powdered specimens made the peak area more difficult to measure. Also, a contribution due to overlapping lines had to be made in the determination of the oxide peak area in the K-LL aluminum spectra of mixed oxide/metal powdered specimens. This is alluded to in Figure 2, where the ^1S Auger state excited in the metal overlaps with the ^1D state excited in the oxide. A DuPont 310 Curve Resolver was used in measuring the peak areas in this study. The error in measuring the areas of the same peak was determined to be less than 5 percent in these studies, even

in cases of unusually large changes in background and even in cases where there was extensive peak overlapping.

The equations used for measuring the oxide thicknesses assume continuous, layered, and homogeneous thin films. It has been shown by Ebel[11] that nearly all of these deviations from the ideally flat, smooth, and homogeneous film structure can cause the observed discrepancies in d_O calculations. The d_O deviations were found to vary with analyzed angular detection, where surface roughness was determined to be the major cause of the observable deviation. Clark et al.[12] also studied the angular dependence of homogeneous and inhomogeneous gold and polymer substrates and thin films. They noted that the intensity ratio of film/substrate was a function of the angle of incidence that the X-ray beam makes with the sample surface. In this study on oxide and carbon thicknesses, the angle of incidence was kept at 45° and the surface roughness was assumed to be constant. This latter assumption is not unreasonable since the samples were all powdered specimens of flaked aluminum and of cuprous oxide with both having particle sizes of less than 10 μm.[8] These thermite samples can be assumed to be infinitely rough with little deviation from specimen to specimen.

The residual gas analysis spectra taken on the vacuum system showed hydrogen, water vapor and carbon monoxide to be the major constituents at a pressure of 2×10^{-8} Torr. A study done by Shiraki et al.[13] on the adsorption of carbon monoxide on clean aluminum films found that both an Al-C type of bond and an Al-O type bond are formed. In our calculations it was assumed that the carbon layer is on top of the initial oxide formed. This need not be true for a freshly sputtered aluminum metal foil. Additionally, it has been shown that the initial oxide growth on a clean aluminum surface is not stoichiometric Al_2O_3 but can consist of suboxides.[14,15] Mean free path values could differ under these circumstances in intensity measurements used to correct for oxide and carbide growth.

4. SUMMARY

XPS data were recorded on the Al 1s, Al 2s and C 1s levels of the thermite components, aluminum metal flakes and cuprous oxide powder. High resolution AES scans were made on the Al K-$L_{2,3}L_{2,3}$ transitions of the thermite components. XPS and AES data were also collected on the thermite blend and on the thermite consolidated pressed pellet. Equations relating the intensity of the photoelectron and Auger peaks to the thickness of the surface contaminants and/or reaction products were developed.

On the aluminum metal flakes, no change in surface oxide or surface carbon levels could be noted for specimens aged at room temperature in dry air. Surface oxide thicknesses of 9.8 Å were measured for the room temperature stored powdered aluminum. Upon increasing the storage temperature to 180°C in dry air, the aluminum oxide thickness increased. At 40 days storage, the oxide was measured to be 13 Å. At 91 and 136 days the oxide was found to remain constant at 13 Å. Carbon contaminant levels were found to decrease upon storage at 180°C from 64 Å for room temperature stored metal to 34 Å for high temperature stored powder.

The largest oxide thicknesses were calculated to be 25 Å on aged thermite powders and 26 Å on aged pressed pellets; minimum carbon contamination was measured to be $\leq$20 Å for these aged samples. It is interesting to note that the aluminum oxide thickness increases in the following order for room temperature aged specimens: Al metal powder (9 Å) < thermite powder (11 Å) < thermite pressed pellet (22 Å).

5. REFERENCES

1. L. D. Haws, M. D. Kelly, and J. H. Mohler, "Consolidated Al/Cu_2O Thermites," Monsanto Research Corporation, Mound Laboratory Report, MLM-2531, Miamisburg, OH 45342.

2. T. N. Wittberg, J. R. Hoenigman, W. E. Moddeman, C. R. Cothern, and M. R. Gulett, J. Vac. Sci. Technol., 15, 348 (1978).

3. C. D. Wagner, Anal. Chem., 49, 1282 (1977).

4. A. Rengan and W. E. Moddeman, "X-Ray Photoelectron Studies on the Thermite Mixture of Aluminum and Cuprous Oxide," University of Dayton Technical Report No. UDRI-TR-77-30, Dayton, OH 45469.

5. T. A. Carlson, W. E. Moddeman, and M. O. Krause, Phys. Rev., A1, 1406 (1970).

6. W. E. Moddeman, "Auger Spectroscopy of Single Gaseous Molecules, Oak Ridge National Laboratory, ORNL-TM-3012, September 1970.

7. W. E. Moddeman, C. R. Cothern, and J. N. Black, J. Environm. Sci., Sept./Oct., 27 (1975).

8. F. P. Mertens, Surf. Sci., 71, 161 (1978).

9. T. A. Carlson and G. E. McGuire, J. Electron Spec. Related Phenom., 1/2, 121 (1974).

10. K. Siegbahn, C. Nordling, A. Fahlman, R. Nordberg, K. Hamrin, J. Hedman, G. Johansson, T. Bergmark, S. Karlsson, I. Lindgren and B. Lindberg, Atomic Molecular and Solid State Structure Studied by Means of Electron Spectroscopy, ESCA (Almquist and Wiksells, Uppsala, Sweden, 1967) p.

11. M. F. Ebel, J. Electron Spec. Related Phonom., 14, 287 (1978).

12. D. T. Clark, A. Dilks, D. Shuttleworth, and H. R. Thomas, J. Electron Spec. Related Phenom., 14, 247 (1978).

13. Y. Shiraki, K. L. I. Kobayashi, and Y. Katayama, Surf. Sci., 77, 458 (1978).

14. S. A. Flodstrom, R. Z. Bachrach, R. S. Baner, and S. B. M. Hagstrom, Phys. Rev. Lett., 37, 1282 (1976).

15. K. L. I. Kobayashi, Y. Shiraki, and Y. Katayama, Surf. Sci., 77, 449 (1978).